Derailment-resistant Performance of Modular Composite Rail Track Slabs

Kaewunruen, Sakdirat; Wang, Yikai; Ngamkhanong, Chayut

DOI:
10.1016/j.engstruct.2018.01.047

Derailment-resistant Performance of Modular Composite Rail Track Slabs

Sakdirat KAEWUNRUEN[1,2], Yikai WANG[1] and Chayut NGAMKHANONG[1]

[1]Department of Civil Engineering, School of Engineering, University of Birmingham, Birmingham B152TT, United Kingdom

[2]Birmingham Centre for Railway Research and Education, School of Engineering, University of Birmingham, Birmingham B152TT, United Kingdom

Abstract: Railway transportation, comprising freight and passenger transport, is the lifeblood of the social economy of a country today, especially for developing countries. Despite over a decade of operations, derailment accidents are among the most frequent accidents for railway transportation and may cause fatally or severe injury to passengers, loss of property and damage to the railway track. Hence, this study focuses predominantly on the structural response and performance evaluation of composite rail track slabs through 3D finite element analysis using ABAQUS. The response and performance of composite track slab subjected to derailment actions has been observed. Material strain-rate properties and impact loads have been introduced to the numerical simulation in order to investigate impact behaviours of composite slabs subjected to derailment loading in explicit dynamic analysis. Based on obtained results, it was found that 45 km/h in the direction of gravity is the limit impact velocity for the designed composite rail track slab. The outcome of this study will improve the design standard and calculation of composite rail track slabs subjected to derailment actions.

Keywords: derailment; impact loading; impact velocity; strain-rate property; composite slab and finite element analysis

1. Introduction

Nowadays, railway transportation, including freight and passenger transport, plays a significant role in the economic development of a region or even a whole country. It is apparent that there are many irreplaceable merits of rail transportation. First, the rail sector performs better financially compared with air or road transportation, which is crucial for developing countries. Second, it can shorten transit time dramatically compared to shipping. Finally, it is adaptable to most geographical situations, so the transport route can be more flexible. However, unexpected train derailment accidents have become a substantial issue. Train derailment is common for both freight and passenger train accidents and it always has disastrous consequences due to its heavy weight and rapid speed [1-5].

According to the *Rail Accident Report: Derailment at Grayrigg* [6], an express passenger train, which was a nine-car, electric, multiple unit, travelling from London Euston to Glasgow, derailed near Grayrigg bridge in Cumbria at the speed of 95 mph (153 km/h) on 23 February 2007 as shown in Fig. 1. This event caused severe damage to the train and injuries to the passengers and driver. One passenger was fatally injured; 28 passengers, the train driver and one other crew member received serious injuries and 58 passengers received minor injuries.

Fig.1: Aerial view of the derailed train from the Grayrigg derailment [6]

Table 1 shows the numbers of unexpected derailment accidents in the USA between 2007 and 2016. It can be clearly seen that more than 1,000 events were observed every year between 2007 and 2016 [7]. As a result, government and related industries should do more to control the risk of train derailments through the design and operation phase, informed by a full understanding of every previous accident. Kaewunruen and Remennikov [8-10] suggested that the impact loading, which has an extremely high magnitude over a short time period, should be considered in the limit states design method.

Year	**2007**	**2008**	**2009**	**2010**	**2011**	**2012**	**2013**	**2014**	**2015**	**2016**
Derailment	1,789	1,370	1,333	1,470	1,294	1,312	1,312	1,321	1,351	1,149

Table 1. Derailments statistics in USA between 2007 and 2016 [7]

Jafarian and Rezvani [11] used a persuasive method called 'fuzzy fault tree analysis' to look for the basic reasons for train derailments. They found that broken rails and lots of technical faults are the main hazards in derailment accidents. Cao et al. [12] suggested that government and related industries should pay particular attention to some specific factors when train derailments occur on bridges rather than on other lines. At present, a new modular composite track slab has been designed to change the conventional structures on railway bridge transoms [13]. Oehlers and Bradford [14-15] revealed that an ideal composite construction involves a combination of concrete with a high compressive strength and high tensile strength steel. Currently, most railway bridge transoms are made up of different kinds of timber. However, there are some shortcomings in timber railway sleepers/transoms, evidenced by their high replacement frequency and rapid deterioration from chemical attack [16]. Manalo et al. also tried to find an alternative material, such as fibre composites, to replace timber. However, the fibre composites material is still in trial stage.

Based on a critical literature review, the derailment resistant capacity of railway track slabs has not been investigated. In particular, the composite track slabs installed over bridge girders are prone to failure under derailment impacts [7, 12, 17]. Thus, this paper aims to establish a 3D finite element modeling in ABAQUS, in order to improve a numerical simulation of a modular composite rail track slab. In this study, sensitivity analysis is also performed in order to evaluate structural capacity considering strain rate effect of composite track slabs under derailment impacts. This is a world first in highlighting the performance of composite rail track slabs under train derailments by considering the effect of strain rate. The insight from this study will improve the design standards and calculations relating to composite rail track slabs, for a better performance and capacity to prevent damage from dynamic load caused by train derailment.

2. Design Methodology

2.1. Design Loading

2.1.1. Dead Load

The thickness of a panel for a railway is restricted to 0.18m and the density of concrete is taken as 2,400 Kg/m^3. In addition, the thickness of the steel sheeting profile bondek section is negligible compared to concrete part and acceleration of gravity (g) is taken as 9.81 m/s^2 [16].

2.1.2. Live Load

A series of general rules of design calculation, such as dynamic effects, centrifugal forces, nosing force and braking force, have been determined in *Part 2: Traffic loads on bridges of BS* EN 1991-2:2003 [19]. This report also introduces some load models to represent distinct train loadings. A model named ‘Load Model 71’ is adopted in this study, which displays a normal static effect of vertical rail traffic loads on mainline railways. Fig. 2. shows characteristic values for vertical loads for Load Model 71. These values shall be multiplied by a factor “α”, which can be either higher or lower than normal traffic, depending on the actions. The characteristic vertical load multiplied by factor α can be called as “Classified vertical load”. In summary, the concentrated 26 force Q_{vk} and the distributed load q_{vk} for Load Model 71 shall be taken as 250 KN and 80 KN/m respectively [19].

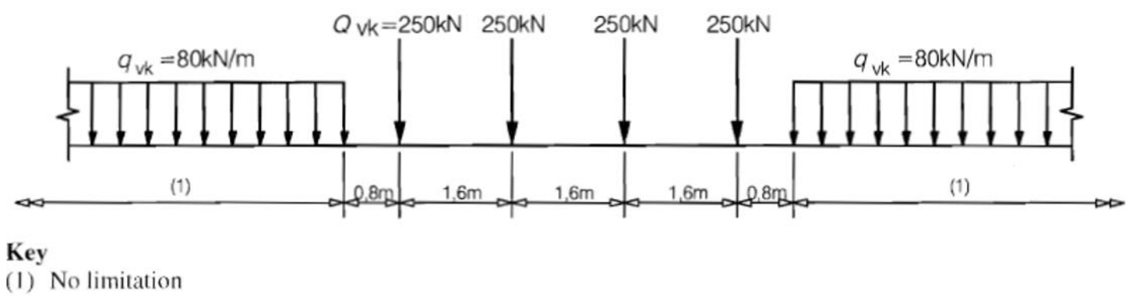

Fig. 2. Load Model 71 and characteristic values for vertical loads [18]

2.1.3. Derailment Actions

Derailment accidents have always been accompanied by huge property damages and casualties. Consequently, derailment action calculations should be adopted in the design phase “as an Accidental Design Situation” [19] in order to minimize the damage to the structure.

There are two specific design situations relating to derailment action on railway bridges that shall be taken into account. Fig. 3a. represents the design situation I, where derailed vehicles are still in the track area, due to the adjacent rail or the containment wall and are preventing the main part failure of the whole structure, is the top priority for designers [19]. Design load Q_{Ald} and q_{Ald} here should be taken as α x 0.7 x LM 71, where LM 71 is 250 kN [19]. Similarly, design Situation II shows another circumstance where derailed vehicles are not in the track area but are on the edge of a bridge, with wheels on one side [19], as shown in Fig. 3b. Designers should pay close attention to the trend of the whole structure overturning or collapsing within Design Situation II. Some local damage is allowed in this circumstance. The equivalent load q_{A2d} shall be taken as α x 1.4 x LM 71 for Design Situation II. For both cases, the characteristic vertical load shall be multiplied by the factor α of 1.1 in terms of derailment action for accidental design situations [20].

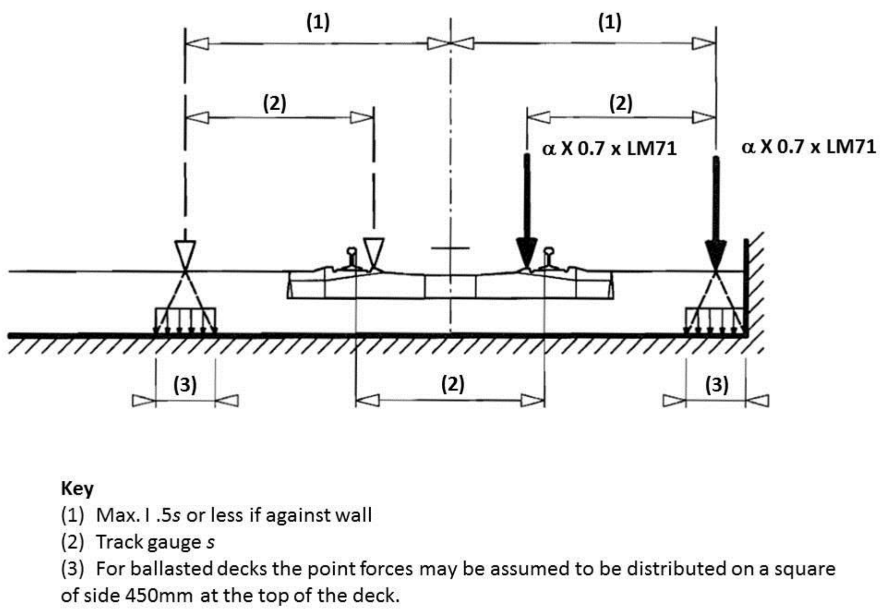

a)

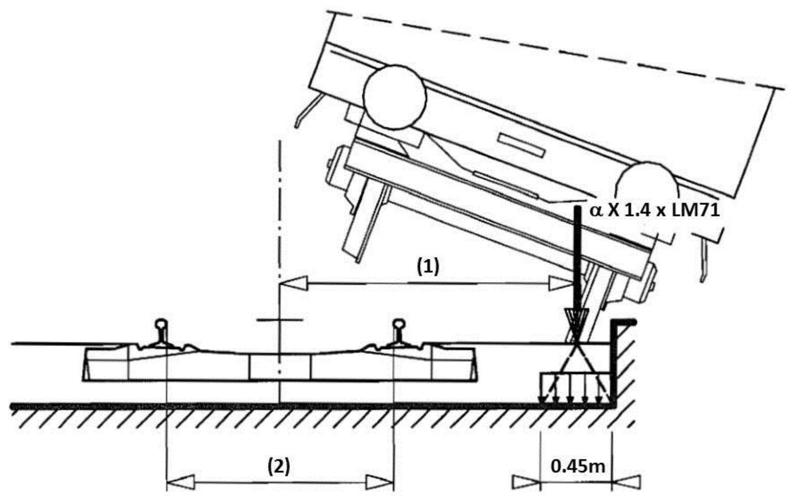

Key
(1) Max. I .5*s* or less if against wall
(2) Track gauge *s*

b)

Fig. 3. a) Design Situation I - equivalent load Q_{Ald} and q_{Ald}

b) Design Situation II - equivalent load q_{A2d} [19]

2.2. Finite Element Modeling

Nowadays, finite element analysis (FEA) is a common approach to simulate the behaviour and response of a structural body and to solve many reality problems in the area of engineering. It can reduce engineers' workload significantly. ABAQUS has been used for this study. The proposed modular panel designs have been carried out and a half model of the whole structure has been introduced for the derailment analysis [12, 21]. In this study, finite element models for a composite rail track slab sitting on bridge girders (stringers) have been developed using ABAQUS and validated against experimental and field data [21-22]. Fig. 4 clearly displays all six parts of the rail track model: concrete, profiled steel sheet, bridge stringer, shear studs, reinforcing steel and wheel [23-27]. The dimensions for the track slab, comprised of concrete and steel parts, are 1,619 mm in length, 600 mm in width and 180 mm in height. Similarly, the dimensions for the bridge stringer are 1,000 mm in length, 260 mm in width for the top segment and 500 mm in height. There are six shear studs, which have a height of 100 mm, in the model that connect the top concrete, profiled steel sheet and bridge stringer as a whole. In addition, four steel reinforcements are used in the concrete to take the tension force and a wheel (modelled as a rigid body) is used in dynamic analysis only. Table 2 displays the boundary conditions of each component.

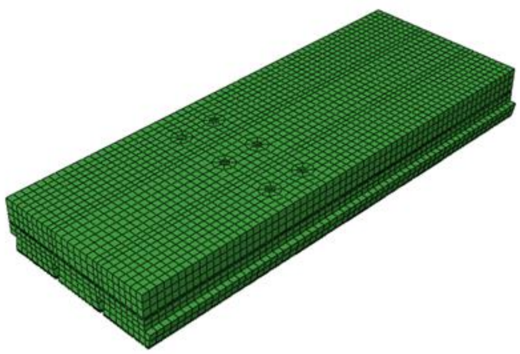

a)

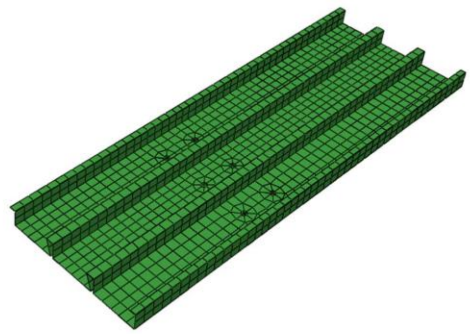

b)

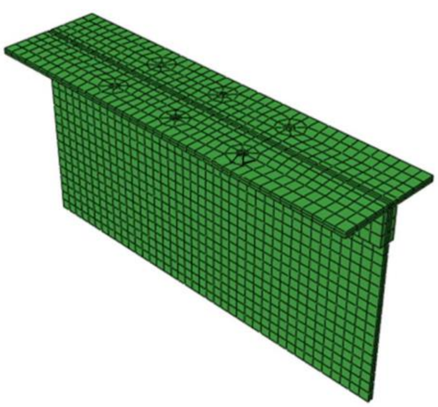

c)

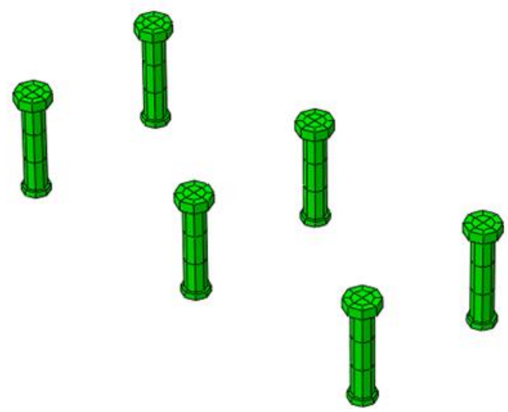

d)

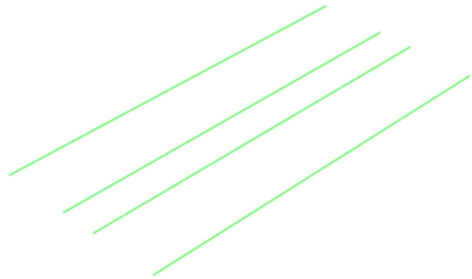

e)

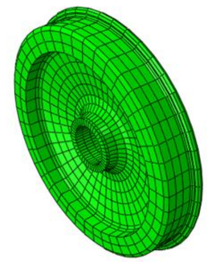

f)

Fig. 4. Main parts of finite element model: (a) Concrete (b) Bondek (c) Bridge Stringer (d) Shear Studs (e) Reinforcing Steel and (f) Wheel

2.3. Contact and Boundary Condition

In term of contact between each component, it is interesting to note that material stiffness is necessary when defining constraint, in order to designate a master surface and a slave surface. The interface types between each element are shown in Fig. 5. It should be noted that the stiffer material is defined as the master surface, whilst the less stiff component is defined as the slave surface. Embedded technique is used as a contact between concrete and reinforced steel, while the contact between the concrete and steel sheet is modelled as a surface to surface with finite sliding, hard contact in the normal direction and a coefficient of friction of 0.5 in the tangential direction [31]. As for the shear studs in the concrete, the interface was modelled as a tie constraint. Tie constraints are considered to be an interface of a shear stud welded to bondek II and bondek II welded to stringer (located below shear studs). Where there is contact between bondek II and stringer outside the shear stud area, surface to surface contact techniques are employed with finite sliding, hard contact in the normal direction and a frictionless surface was assumed in the tangential direction.

The cut edges of the supporting stringers and the nodes of this surface have been assigned encastre boundary conditions (fully fixed in the three degrees of both translational and rotational freedom).

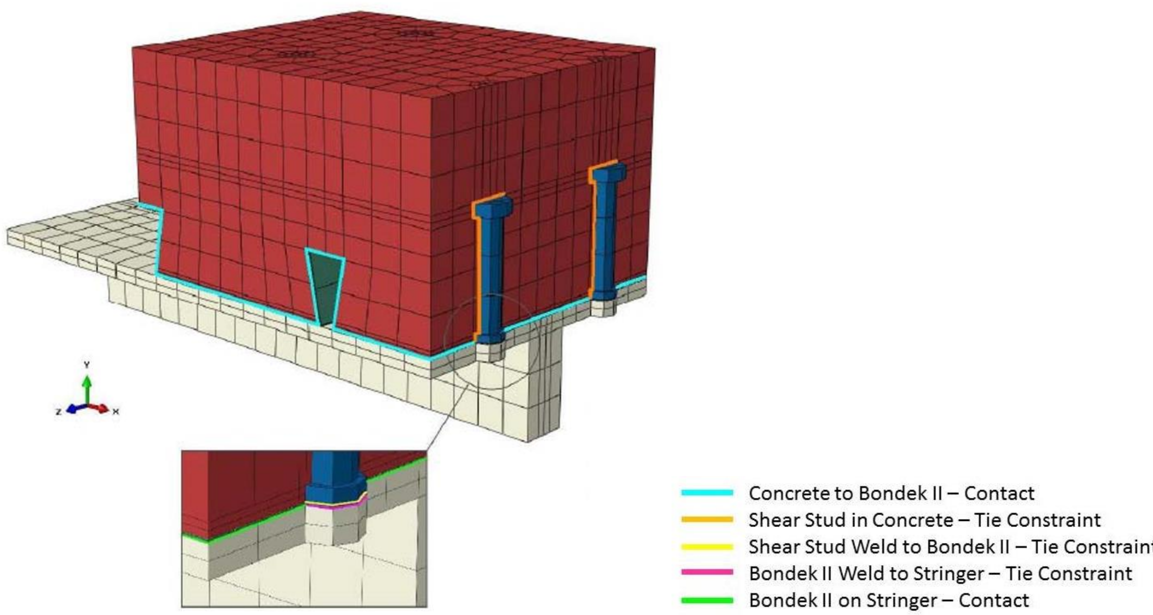

Fig. 5. Contact and interactions between composite slab panel materials [22]

Interface	**Interface type**	**Master surface**	**Slave surface**
Reinforcing steel in Concrete	Embedded	Reinforcing steel	Concrete
Concrete to Bondek II	Surface to surface contact	Bondek II	Concrete
Shear stud in concrete	Tie constraint	Shear stud	Concrete
Shear stud welded to Bondek II	Tie constraint	Bondek II	Shear stud
Bondek II welded to stringer	Tie constraint	Bondek II	Stringer
Bondek II on stringer	Surface to surface contact	Bondek II	Stringer

Table 2. Contacts and interface type between composite panel elements [22]

2.4. Material Properties

2.4.1. Static Analysis

2.4.1.1. Concrete

Concrete is an indispensable part of the composite rail track slab due to its high compressive strength. For static analysis, the elastic plastic method has been chosen for concrete, and 50 MPa was taken as the compressive strength (f_c'). Fig. 6a shows the typical stress strain curve for concrete; there are two main parts in the curve. In this study, $f_{tension}$ is 5.94 MPa when the concrete compressive strength is 50 MPa and is when the concrete in the tension area will begin to crack if the stress at the tension zone exceeds the maximum cracking stress $f_{tension}$.

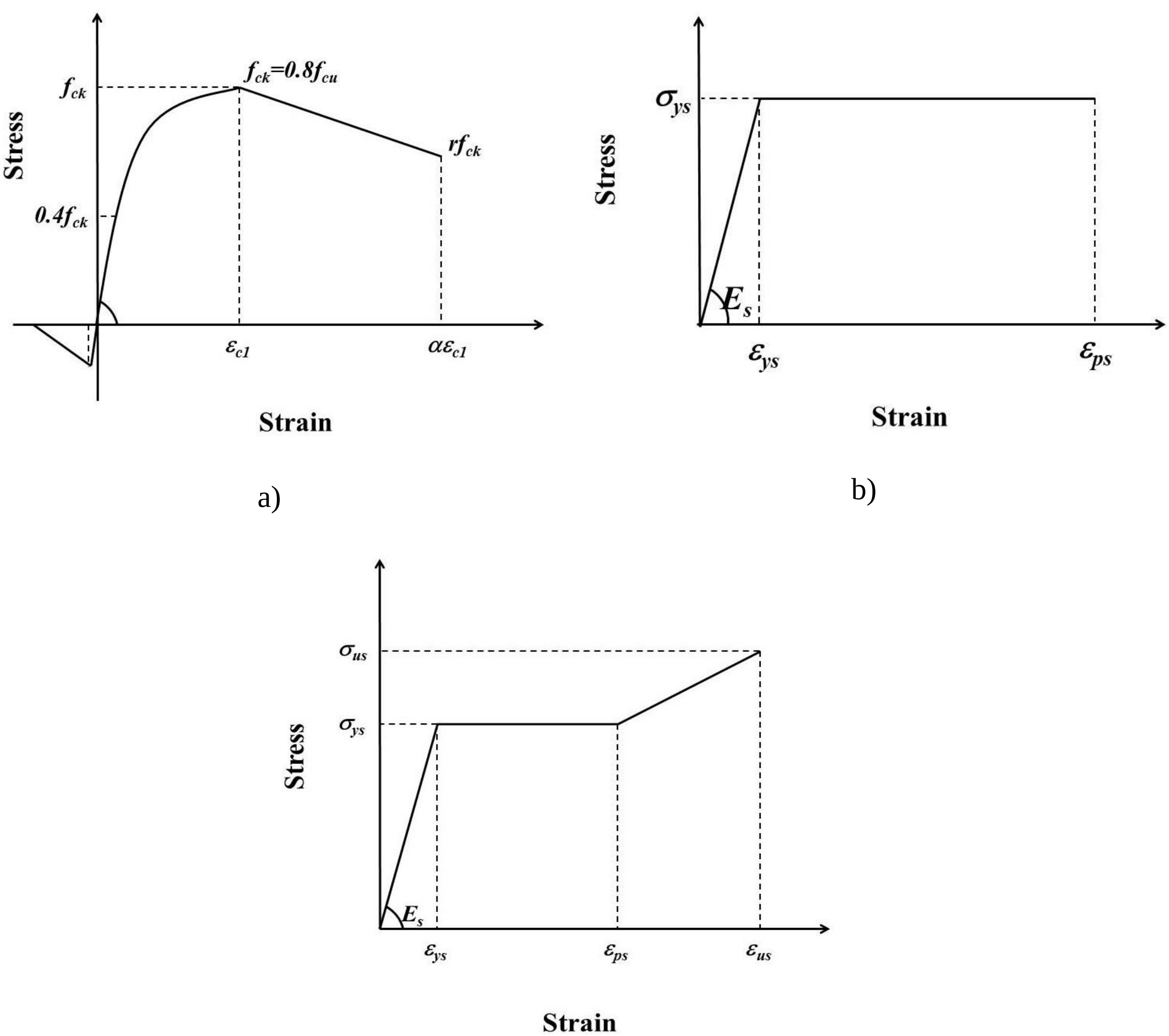

c)

Fig. 6. a) Typical stress strain curve for concrete (Nguyen and Kim [28]) b) Typical bilinear stress strain curve for steel (Anandavalli et al. [29]) c) Classic tri-linear stress strain curve (Haghinejada and Nematzadeh [30])

2.4.1.2. Steel

Most parts of the model are steel elements, such as the profiled steel sheet, bridge stringer, headed shear studs, reinforcing steel and wheel. An elastic plastic method was also selected here for all steel elements and for the concrete. Moreover, two different types of stress strain curve were used for the steel elements in static analysis. The specific material properties for different steel elements have been shown in Table 2 [31-33]. First, a typical bilinear stress strain curve is adopted for the profiled steel sheeting and shear studs. According to Fig. 6b there are only two stages for profiled steel sheeting and shear studs: elastic and yield stages. In addition, there is the yield stress and the yield strain. Second, a classic tri-linear stress strain curve is used here for the bridge stringer and reinforcing steel in the model. As shown in Fig. 6c there are three steps named elastic, yield and strain hardening for bridge stringers and reinforcing steel. The parameters of the steel materials can be found in Table 3.

Element	**Yield Stress f_y (MPa)**	**σ_{us} (MPa)**	**ε_{ps}**	**ε_{us}**
Stringer	300	$1.28\sigma_{ys}$	$10\varepsilon_{ys}$	$30\varepsilon_{ys}$
Reinforcing Steel	500	$1.28\sigma_{ys}$	$9\varepsilon_{ys}$	$40\varepsilon_{ys}$
Bondek	550	N/A	$20\varepsilon_{ys}$	N/A
Shear Studs	420	N/A	$25\varepsilon_{ys}$	N/A

Table 3. Steel element material properties for static analysis

2.4.2. Dynamic Analysis

Variations in the dimensions under time-dependent stress are a common phenomenon for most materials. There are two kinds of deformation characteristics that exist under stress. Elastic behaviour is a deformation that can be returned to its initial shape and plastic behaviour can leave permanent deformations when the stress is lifted. The strain-rate properties of materials also hinges on the load characteristics. A derailment load is an impact force caused by the train wheels suddenly hitting the composite rail track slab during the derailment accident. It is crucial for designers to consider the change in specific material strength with different strain rates associated with the impact loading. Strain-rate behaviours of concrete and steel will be introduced separately.

2.4.2.1. Concrete

Concrete is the first contact part of the slab when an unexpected derailment accident occurs, so the strain rate property of concrete is crucial. Using the research presented by Wakui and Okuda [34], the dynamic stress strain curves in different strain rates shall be computed. The dynamic compressive strength of concrete df'_c can be determined in Equation (1).

$$df'_c/sf'_c = 1.49 + 0.268(log\dot{\varepsilon}) + 0.035\,(log\dot{\varepsilon})^2 \quad (1)$$

Where sf'_c is the static compressive strength of concrete

$\dot{\varepsilon}$ is the strain rate

For this study, the static compressive strength of concrete sf'_c is taken as 50 MPa (characteristic strength), which was introduced in section 2.3.1.1. The dynamic strength complies with the nature of materials undergoing transient loading [9]. In addition, two intermediate strain rates (5 s^{-1} and 25 s^{-1}) and three high strain rates (300 s^{-1}, 500 s^{-1} and 850 s^{-1}) have been adopted in this study. The higher the strain rate is, the greater the dynamic stress is at the same strain. According to Equation (1), the dynamic ultimate compressive strength of concrete can be calculated as 128.8 MPa.

2.4.2.2. Steel

Recently, Forni et. al. [35] conducted a study on the strain rate performance of S355 steel, which is currently used in composite construction. Five distinct strain rates (5 s^{-1}, 25 s^{-1}, 300 s^{-1}, 500 s^{-1} and 850 s^{-1}) were used for their experiments. It is found that the strain rates exactly coincide with the concrete property described in section 2.3.2.1. It is found that the dynamic ultimate strength of steel at the greatest strain rate in this project is 695 MPa.

3. Result and Discussion

The finite element analysis results from the composite rail track slab subject to the derailment loads are then discussed hereafter. Critical elements in key areas will be highlighted in order to portray the dynamic performance of the modular composite track slabs.

3.1. Static Analysis

3.1.1. Loading condition

Two different design circumstances in European Code should be considered separately.

For Design Situation I, two concentrated forces act on the top concrete of the composite slab. Moreover, these loads equal α x 0.7 x LM 71, where LM 71 is 250 kN and α is adopted as 1.1, so the two concentrated forces = 1.1 x 0.7 x 250 kN = 192.5 kN respectively.

Pressure is then selected in ABAQUS as the loading type because it is a three dimensional model. Fig. 7a shows the exact contact area between a train wheel and top concrete. It is determined by the standard wheel dimension and a 30 degree segment of the train wheel [31-33].

The contact area is thus taken as 0.033 m^2, therefore the pressure relating to the Design Situation I = 192.5 kN / 0.033 m^2 = 5834 KPa = 5.834 MPa.

Fig. 7b. shows the exact load location for Design Situation II, where the ultimate limit state method is used. As a result, the limit point load for Design Situation II has been determined as 153.45 KN, after a series of attempts in ABAQUS. Therefore, the pressure concerning Design Situation II = 153.45 kN / 0.033 m^2 = 4650 kPa = 4.65 MPa. Moreover, the modified RIKS method has been selected here in ABAQUS, which, means the pressure is applied in the model incrementally.

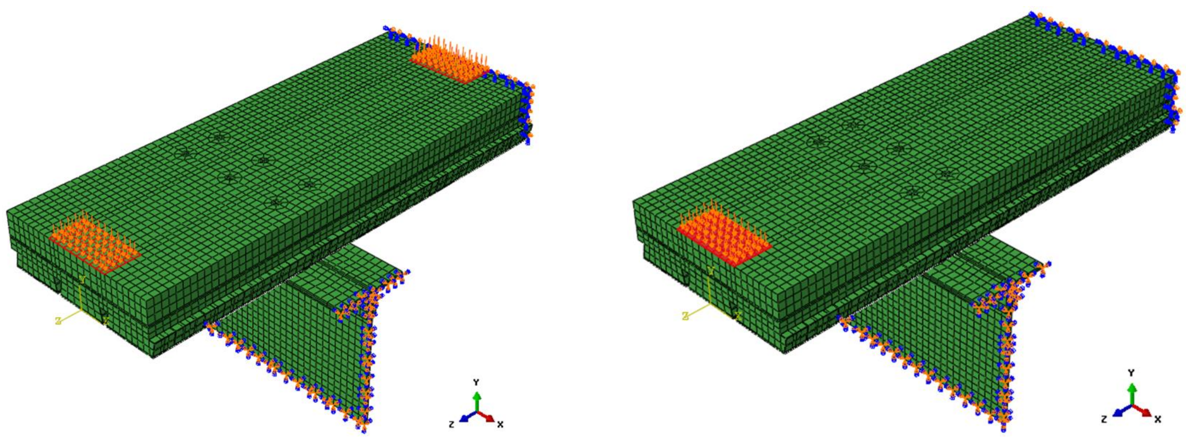

a) b)

Fig.7. Load application plan for a) Design Situation I b) Design Situation II

3.1.2. Static Response

3.1.2.1. Design Situation I

The deformation shape for Design Situation I is demonstrated in Fig. 8. There are four individual parts that need to be checked in the model: concrete, bondek, headed shear studs and bridge stringer. Four critical locations considering the worst stress resultants in concrete have been determined and highlighted.

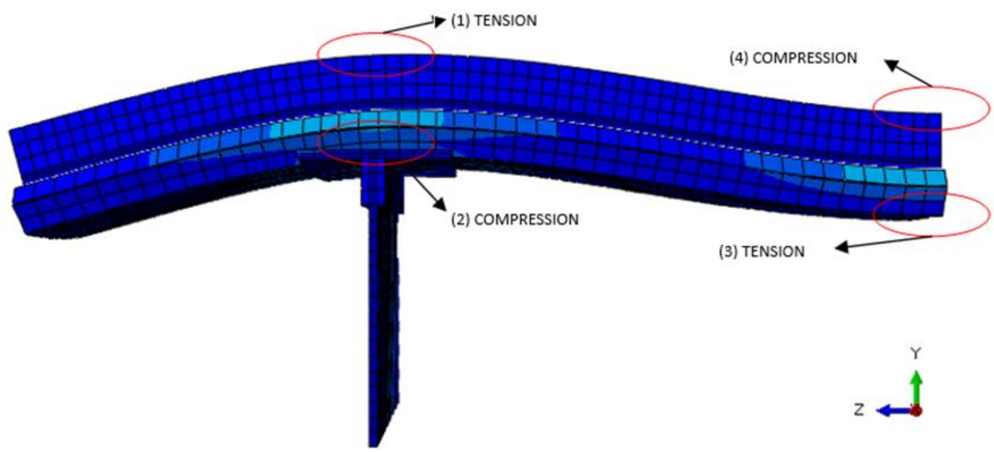

Fig.8 Critical location for Design Situation I

The critical tension zones are located in areas (1) and (3). The maximum stresses here are 20.7 MPa and 21.7 MPa, for concrete in tension zones respectively, when the ultimate cracking stress $f_{tension}$ in this study is 5.94 MPa. Then, the performance of reinforcing steel bars associated with the areas (1) and (3) need to be observed, because they start to sustain the tensile force. The maximum stress of reinforcing steel in the areas (1) and (3) are 40.7MPa and 6.2 MPa respectively, which is clearly below the ultimate strength of tensile (500 MPa). Moreover, area (3) is at the bottom of the concrete and interacts with the profiled steel sheet below, which can be another element that can resist an external stress. Hence, this area is in a safe situation.

In term of compression zones located in area (1) and (3), the maximum compressive stresses are 48.6 MPa and 17.5 MPa, which is less than yield strength (50 MPa). Hence, these areas are in safe situation as well as bondek, shear stud and bridge stringer as shown in Table 4.

Element	Location	Maximum stress (MPa)	Yield Strength (MPa)	Design Ratio
Slab (Concrete)	(1) Tension	21	6	0.29
Slab (Steel)	(1) Tension	41	500	12.29
Slab (Concrete)	(2) Compression	49	50	1.03
Slab (Concrete)	(3) Tension	22	6	0.27
Slab (Steel)	(3) Tension	6	500	80.65

Slab (Concrete)	(4) Compression	18	50	2.86
Bondek	Bondek 1	236	550	2.33
Shear stud	Shear stud 1	238	420	1.76
Bridge stringer	Bridge stringer 1	138	300	2.17

Table 4. Maximum stress in critical zone for Design Situation I

3.1.2.2. Design Situation II

Fig. 9 shows the deformation shape under the derailment load concerning Design Situation II. There are four individual parts (concrete, bondek, shear studs and bridge stringer), which need to be evaluated as follows.

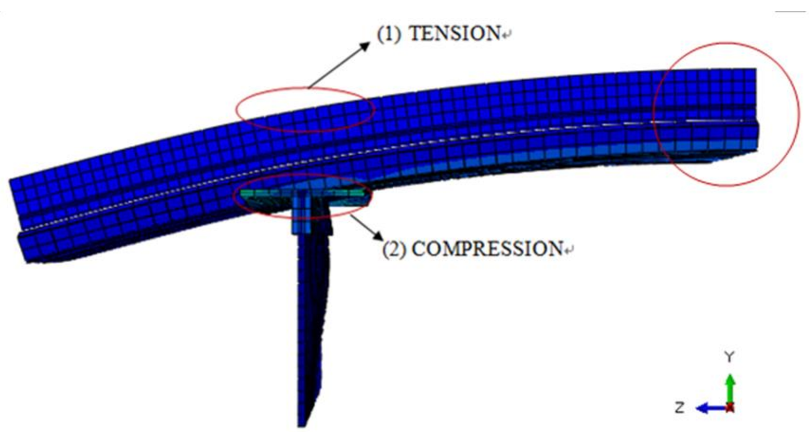

Fig. 9. Critical location for Design Situation II

For Design Situation II, the critical tension zone is located in area (1), as shown in Fig. 9. The maximum stress here is 20.7 MPa, which is more than the ultimate cracking stress $f_{tension}$ (5.94 MPa). Then, the performance of reinforcing steel bars associated with the area (1) needs to be observed because they start to sustain the tensile force. The maximum stress of reinforcing steel in the area (1) is 6.2 MPa, which is obviously below the ultimate strength of tensile force (500MPa). Hence, there is no damage in this area. The compression zone is located in area (2). The maximum compressive stress is 47.7 MPa, which is less than yield strength (50 MPa).

Hence, these area are safe under Situation II, as well as bondek, shear studs and bridge stringer. Maximum stresses in the critical zone for Design Situation II are shown in Table 5.

Element	Location	Maximum stress (MPa)	Yield Strength (MPa)	Design Ratio
Slab (Concrete)	(1) Tension	15	6	0.40
Slab (Steel)	(1) Tension	34	500	14.84
Slab (Concrete)	(2) Compression	48	50	1.05
Bondek	Bondek 1	390	550	1.41
Shear stud	Shear stud 1	384	420	1.09
Bridge stringer	Bridge stringer 1	240	300	1.25

Table 5. Maximum stress in the critical zone for Design Situation II

Although, there is no damage in this situation, the maximum stress of most parts under Design Situation II, especially the steel elements, is greater than that under Design Situation I, so the Design Situation II is more dangerous when a derailment accident occurs. This is the reason why the total force applied at the wheel location for Design Situation II is much smaller. In addition, all parts of the model are in a safe situation and maximum design action is below the design capacity, hence the model satisfies the derailment load according to Design Situation II, which is one concentrated force of 153.45 KN applied on the end of the composite rail track slab. After comparing two different derailment situations in BS EN 1991-2:2003 [18], Design Situation II is the worst case, so Design Situation II has been chosen for dynamic analysis.

3.2. Dynamic Analysis

3.2.1. Loading Condition

Impact loading is a high magnitude force or a shock pulse applied over a short period of time. In this study, the derailment loads are generated only when an unexpected train accident occurs and the first interaction between train wheels from derailed vehicles and the track slab surface is considered. In a real situation [5], a train wheel axle can break and the train can derail at slow to moderate speeds. In such cases, the wheel can nearly vertically drop directly to the track slab.

Hence, impact loading should be simulated and strain-rate behaviours are more appropriate for this investigation. As such, a predefined field (or impact object) is created in ABAQUS to simulate impact loading. The region of the predefined field is the whole wheel in this study, and the velocity has been arranged at the direction of gravity (-V2 in ABAQUS). For initial studies, the drop velocity was selected as 5 km/h to a limit impact velocity to determine the ultimate capacity of the composite track slab. The detailed velocity direction and locations are shown in Fig. 10. After increasing the impact speeds, the limit impact velocity was determined at the magnitude of 45 km/h, due to the design capacity. This limit velocity is the vertical projection of the moving wheel (often, the other longitudinal projection is negligible through the rolling motion of the wheel). Note that the total mass of train has already been transferred to the wheel through the axle (by manually adding mass to the wheel model).

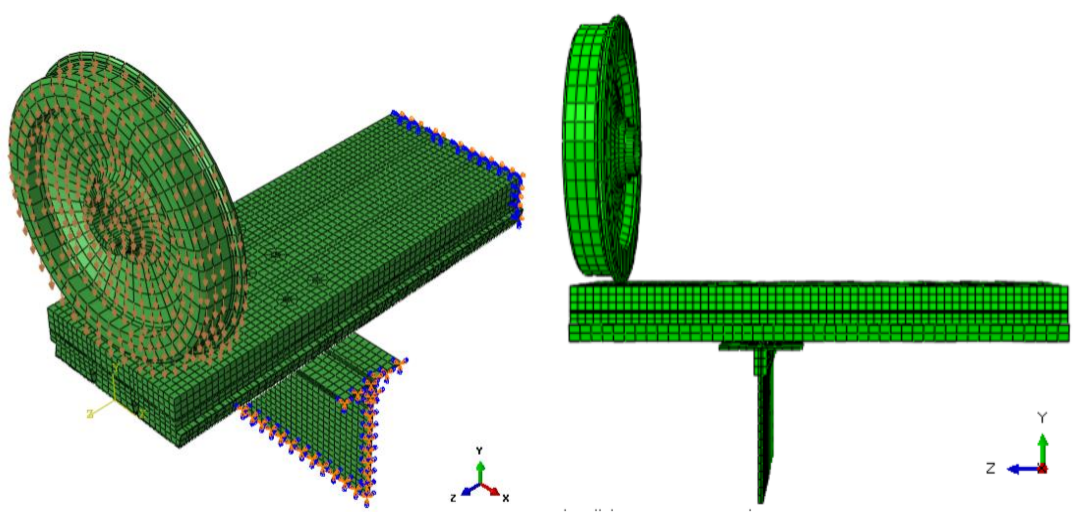

Fig. 10. Three-dimensional model with a train wheel in dynamic analysis

The relationship between the time duration and contact force of the corresponding critical node in the top concrete surface is shown in Fig. 10. The maximum contact force in concrete surface is 20.3 kN at 0.0005 S, which is the first step time in ABAQUS, except the initial situation. Hence, the maximum force is formed in the first contact moment in a derailment accident. From the graph in Fig. 11, three representative peak points have been selected. The magnitude of force shows a downward trend and decreases significantly over time. In addition, the impact loading has disappeared at 0.012 S, which means that the train wheel is removed from the slab area.

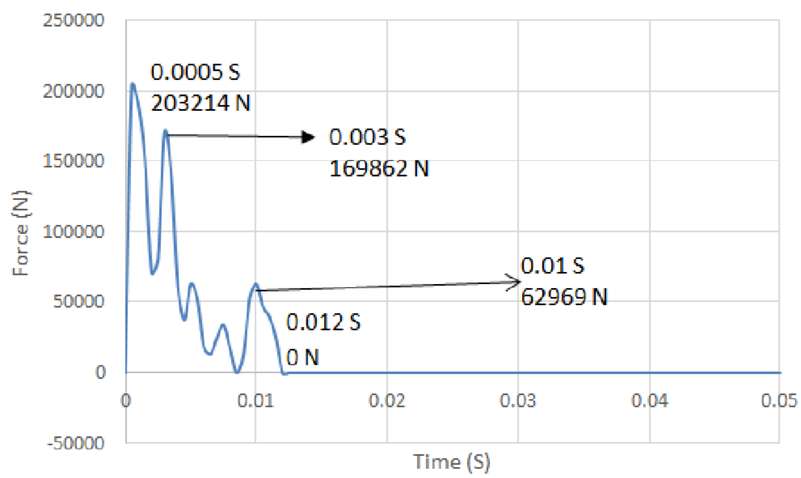

Fig.11. Contact force in top concrete surface

3.2.2. Dynamic Response

The dynamic responses of four individual parts (concrete, bondek, shear studs and bridge stringer) are investigated as follows.

3.2.2.1. Concrete

There are four critical elements for the concrete segment, as shown in Fig. 12a. Fig. 12b shows the exact location of the critical element selected for concrete in area (1). A graph showing the relationship between the average stress of the corresponding concrete element and time is presented in Fig. 12c. It can be observed that the impact loading plays an important role in the changing of stress here. Moreover, the maximum compressive stresses in areas (1) and (4) are 115 MPa and 90 MPa respectively, which is less than the dynamic ultimate compressive strength of concrete (128.8 MPa). Therefore, these areas are within a safe situation.

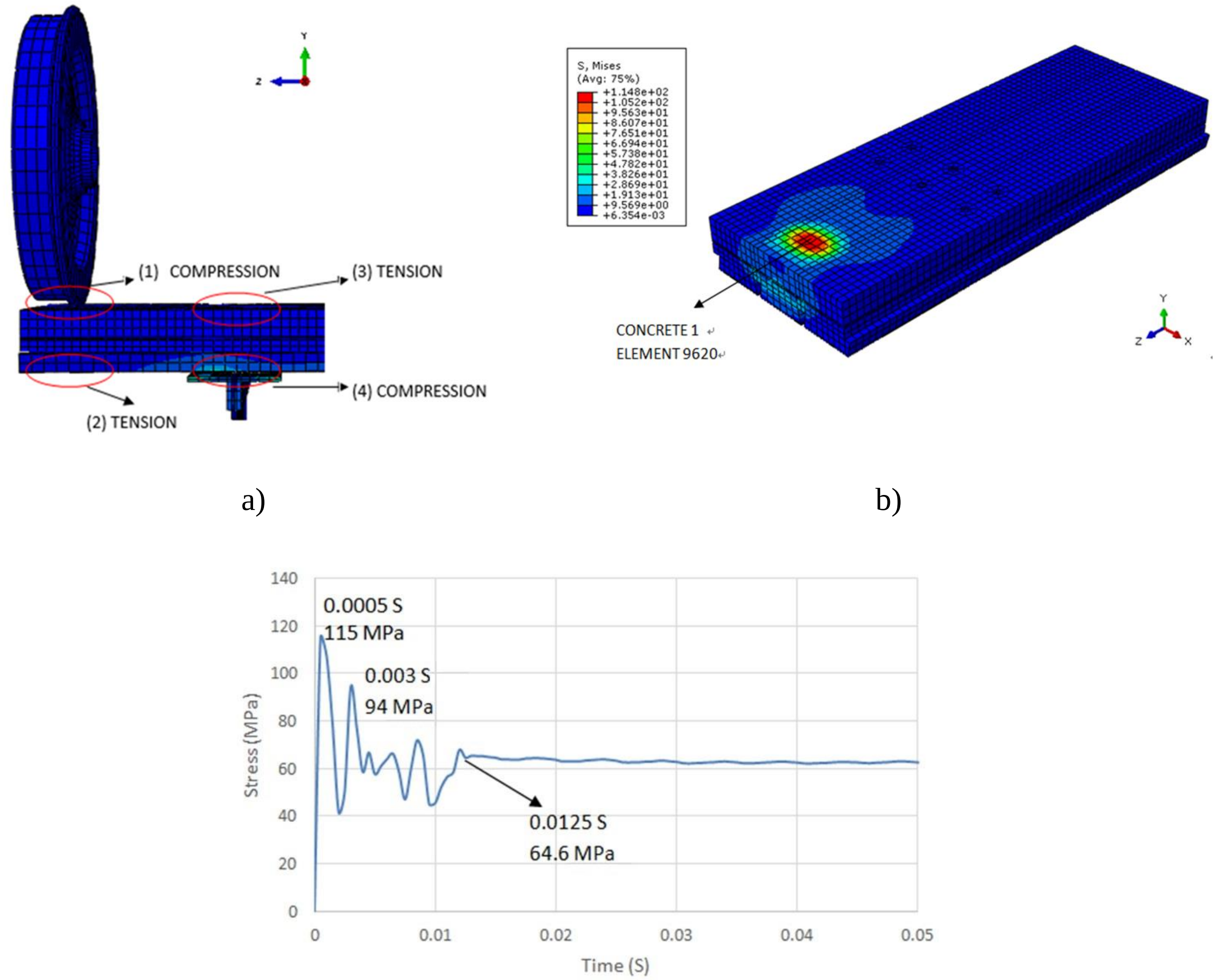

c)

Fig. 12. a) Critical zones in top concrete b) The exact location of critical element selected for concrete in area (1) c) Dynamic stress response in area (1)

In terms of tension area, the critical zones are located in areas (2) and (3), as shown in Fig. 11. The maximum stresses here are 20.5 MPa and 70 MPa respectively, when the ultimate cracking stress $f_{tension}$ in this study is 5.94 MPa, which is less than the maximum stress in both areas. Then, the performance of reinforcing steel bars associated with the areas (2) and (3) need to be observed, since they start to sustain tensile force. The maximum stresses of reinforcing steel in the areas (2) and (3) are 367.5 MPa and 359.5 MPa respectively, which is less than the ultimate strength of reinforcing steel (695 MPa). As a result, these areas have not exceeded the critical zone. Moreover, area (2) is located at the bottom of the concrete and interacts with the profiled steel sheet below it, which can be another element to resist an external stress. However, it is clear that there is no damage in these areas.

3.2.2.2. Steel

Stress distribution situations for the profiled steel sheet (Bondek), sheer studs and bridge stringer have been shown in Fig. 13. The maximum stresses of the profiled steel sheet (Bondek), shear studs and bridge stringer are below the ultimate tensile strength, as shown in Table 6. As a consequence, these areas have not exceeded the critical yielding stress.

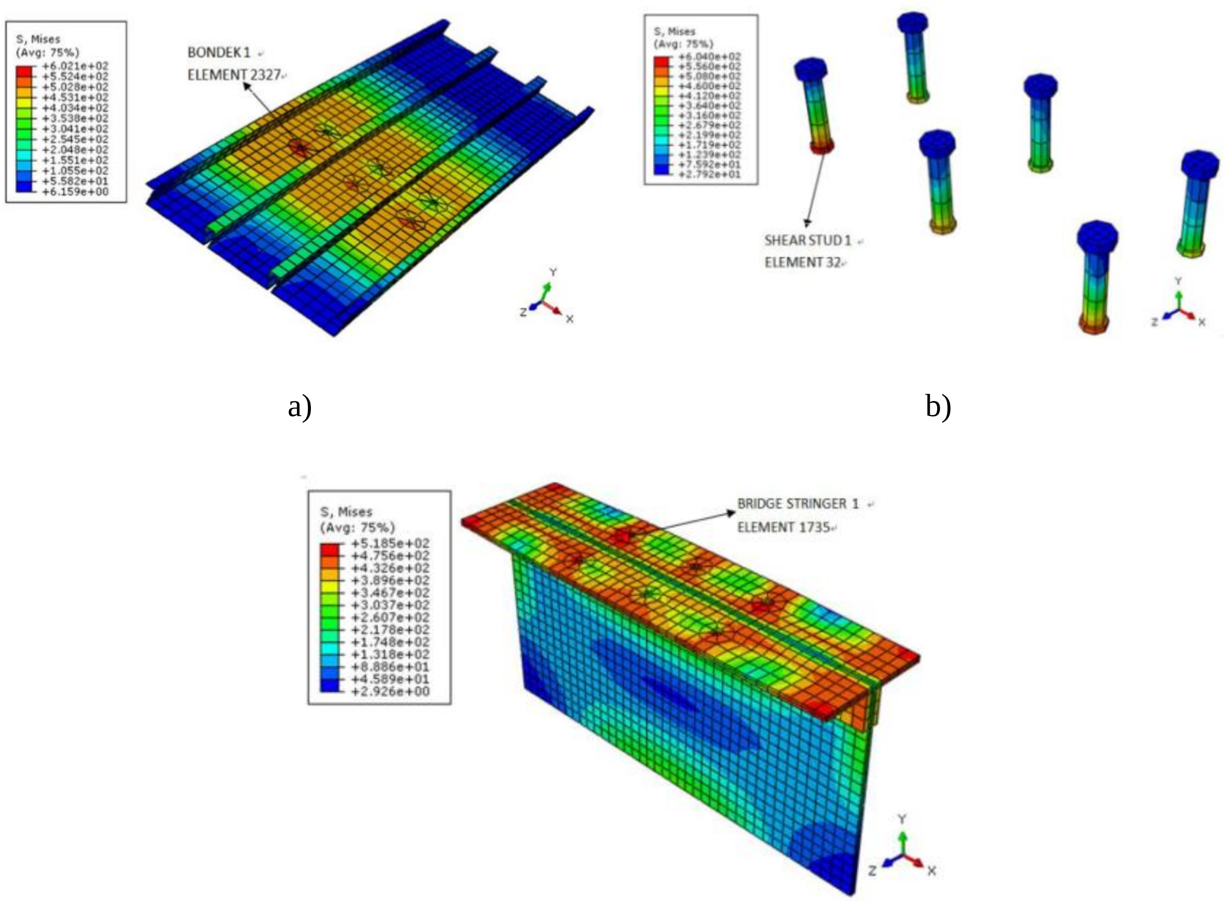

c)

Fig. 13. Dynamic performance of track slab system a) Bondek b) Shear stud c) Bridge stringer

Element	Location	Maximum stress (MPa)	Yield Strength (MPa)	Design Ratio
Slab (Concrete)	(1) Compression	115	129	1.12
Slab (Concrete)	(2) Tension	21	6	0.29
Slab (Steel)	(2) Tension	368	695	1.89
Slab (Concrete)	(3) Tension	70	6	0.08
Slab (Steel)	(3) Tension	360	695	1.93
Slab (Concrete)	(4) Compression	95	129	1.36
Bondek	Bondek 1	236	695	2.94
Shear stud	Shear stud 1	238	695	2.92
Bridge stringer	Bridge stringer 1	138	695	5.04

Table 6. Maximum stress in critical zone for impact loading

The limit impact velocity, which is 45 km/h (-12500 mm/s in ABAQUS), and materials' strain rate properties have been adopted in the dynamic analysis. The largest contact force on the top concrete surface due to the impact velocity of the train wheel is 20.3 kN, which occurred at 0.0005 S and all individual parts in the model did not yield, snap or crush under the impact of derailment loading. Moreover, the maximum bending moment is less than the design capacity. As a result, the whole structure has satisfied the impact speed at 45 km/h.

3.3. Comparative Evaluation

In this comparative evaluation, the elastic plastic properties without materials' strain rate effects are used to predict the behaviour of composite track slab in a similar manner of the model used by Macri et al. [35]. The aim is to compare the stress strain behaviours with and without strain rate effects. In this comparative study, the drop velocity of 30 km/h was found to be the limit impact speed. Table 7 summarizes the maximum stresses of critical elements selected in each individual part with the corresponding material yield strengths under the limit impact speed.

Element	Location	Maximum	Yield Strength	Design Ratio

		Stress (MPa)	(MPa)	
Slab (Concrete)	(1) Compression	47	50	1.06
Slab (Concrete)	(2) Tension	48	6	0.12
Slab (Steel)	(2) Tension	205	500	2.44
Slab (Concrete)	(3) Tension	45	6	0.13
Slab (Steel)	(3) Tension	338	500	1.48
Slab (Concrete)	(4) Compression	43	50	1.16
Bondek	Bondek 1	550	550	1.00
Shear stud	Shear stud 1	420	420	1.00
Bridge stringer	Bridge stringer 1	300	300	1.00

Table 7. Maximum stress in critical zone for contrast experiment

In contrast, the finite element analysis results of the whole track slab model subjected to impact loading, and the material strain-rate properties demonstrated earlier, show that that the speed of 45 km/h is the limit impact velocity and the whole structure is still in a safe situation under the limit impact velocity. Note that this comparative study has used ABAQUS and the three dimensional models for comparison have been established in a manner based on the previous research presented by Macri et al. [35]. This implies that the strain rate properties of materials can significantly improve the track slab performance under derailment impacts, compared with those derived from the normal elastic plastic method.

In addition, Fig. 14. demonstrates the derailment impact spectra related to unexpected derailment actions on the railway composite track slabs. To develop these spectra, a series of impact velocities have been selected as the impacting limit speed and then corresponding critical design ratios (lowest) have been evaluated. The relationship between the design ratio and impact velocity for the composite rail track slabs subjected to derailment accidents can be derived, as shown in Fig. 14. It is important to note that the area under the curve filled with red lines demonstrates the safe situation (where there is no yielding, no crush, nor snap of structural materials) for the whole structure under derailment loading conditions.

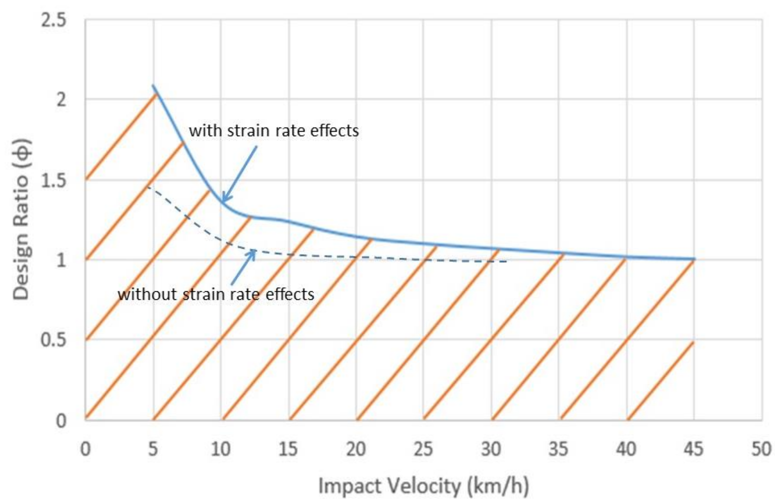

Fig. 14. Design ratio to impact velocity relationship of a composite slab in a derailment accident

4. Conclusion

Railway transportation, including both freight and passenger transport, is an important catalyst for growing the social economy of a country, especially for developing countries. At present, derailment accidents are among the most frequent accidents for railway transportation all over the world. The consequences of derailments are not only the temporary interruption of railway lines but also the varying severity of personnel and property losses. Therefore, this paper focuses predominantly on the structural response and the performance evaluation of the composite rail track slabs associated with derailments through 3D finite element analysis (FEA).

It should be noted that the performance of composite rail track slabs have not been investigated in recent studies. In this research, the model has been developed and validated using ABAQUS. Material strain-rate properties and impact loading have been applied to the numerical simulation simultaneously, in order to improve the impact behaviour of composite slabs subjected to derailment loading in an explicit dynamic analysis. The response and performance of composite track slabs, under two design situations, related to derailment actions has been evaluated. Based on the results obtained, it was noted that the speed of 45 km/h in the direction of gravity is the limit impact velocity for the designed composite rail track slabs considering strain rate effects. Moreover, a comparative study using ABAQUS has been taken in to account order to identify the performance difference between data derived from the elastic plastic material models and material strain-rate properties.

Without the strain-rate effect consideration, the limit impact velocity is 30 km/h using elastic plastic material models. The comparative study also demonstrates that the numerical simulations without strain-rate effects are relatively more conservative than those with strain-rate effects. This paper is a world first in investigating the performance of composite railway track slabs subjected to derailment action. However, experiments also need to be carried out under impact loads in order to obtain an accurate strain-rate of materials.

Acknowledgements

The authors are sincerely grateful to the European Commission for the financial sponsorship of the H2020-RISE Project No. 691135 "RISEN: Rail Infrastructure Systems Engineering Network," which enables a global research network that tackles the huge challenge in railway infrastructure resilience and advanced sensing in extreme environments (www.risen2rail.eu) [37]. The authors would like to acknowledge CEMEX, Network Rail, and other industrial partners, who provided technical assistance throughout this study.

References

[1] Liu X, Barkan C, Saat M. Analysis of Derailments by Accident Cause. Transportation Research Record: Journal of the Transportation Research Board; 2016, 2261, p.178-185.

[2] Liu X, Saat M, Barkan C. Analysis of Causes of Major Train Derailment and Their Effect on Accident Rates. Transportation Research Record: Journal of the Transportation Research Board; 2012, 2289, p.154-163.

[3] Liu X, Saat M, Barkan C. Analysis of Causes of Major Train Derailment and Their Effect on Accident Rates. Transportation Research Record: Journal of the Transportation Research Board; 2012, 2289, p.154-163.

[4] Matias S. NUMERICAL MODELING AND DESIGN OF SLAB TRACKS. University of Lisbon; 2015.

[5] Australian Transport Safety Bureau. Derailment of Sydney Trains Passenger Train 602M. Australian Transport Safety Bureau; 2015.

[6] RAIB. Rail Accident Report Derailment at Grayrigg 23 February 2007. The Rail Accident Investigation Branch, Department for Transport; 2011.

[7] Federal Railroad Administration (FRA). TOTAL ACCIDENTS/INCIDENTS, JAN-DEC. http://safetydata.fra.dot.gov

[8] Remennikov A M, Kaewunruen S. ‘A review of loading conditions for railway track structures due to train and track vertical interaction’, Structural Control and Health Monitoring ; 2008, 15 (2), p.207-234.

[9] Kaewunruen S, Remennikov A. Impact capacity of railway prestressed concrete sleepers. Engineering Failure Analysis; 2009, 16(5), p.1520-1532.

[10] Kaewunruen S, Remennikov A. Experiments into impact behaviour of railway prestressed concrete sleepers, Engineering Failure Analysis; 2011, 18(8), p.2305–2315.

[11] Jafarian E, Rezvani M. Application of fuzzy fault tree analysis for evaluation of railway safety risks: an evaluation of root causes for passenger train derailment. Proceedings of the

Institution of Mechanical Engineers, Part F: Journal of Rail and Rapid Transit; 2011, 226(1), p.14-25.

[12] Cao S, Chen R, Tang Z, Xiao X, Hu H, Tang S, Liu Y, Gao R. Comparison Analysis of Train Derailment between Bridges and Lines. AMM; 2013, 423-426, p.2941-2945.

[13] Kaewunruen S, Griffin DWP, Mirza O, Kwok K, Resilience-based design of precast steel-concrete composites for railway track slabs, Proceedings of the 13th International Railway Engineering Conference, Edinburgh, UK, June 30 - July 1, 2015.

[14] Oehlers D, Bradford M. Composite steel and concrete structural members. Kidlington, Oxford, U.K.: Pergamon; 1995.

[15] Oehlers D, Bradford M. Elementary behaviour of composite steel and concrete structural members. Oxford: Butterworth-Heinemann; 1999.

[16] Manalo A, Aravinthan T, Karunasena W, Ticoalu A. A review of alternative materials for replacing existing timber sleepers. Composite Structures; 2010, 92(3), p.603-611.

[17] Griffin DWP, Mirza O, Kwok K, Kaewunruen S. Finite Element Modelling of Modular Precast Composites for Railway Track Support Structure: A Battle to Save Sydney Harbour Bridge, Australian Journal of Structural Engineering; 2015, 16 (2), p.150-168.

[18] Macri S, Devic A, Asmaro S. Sydney Harbour Bridge: Railway Impact Loadings on Composite Steel-Concrete Transoms. Bachelor. University of Western Sydney; 2015.

[19] British Standards Institution. BS EN 1991-2:2003. Eurocode 1: Actions on structures. BSI; 2010.

[20] British Standards Institution. NA to BS EN 1991-2:2003. UK National Annex to Eurocode 1: Actions on structures. BSI., 2008.

[21] Mirza O, Kaewunruen S, Kwok K, Griffin DWP, Design and modelling of pre-cast steel-concrete composites for resilient railway track slabs, Steel & Composite Structures, An International Journal, 2016, 22 (3), 537-565.

[22] Kimani SK, Kaewunruen S. Free vibrations of pre-cast modular steel-concrete composites railway track slabs, Steel and Comp Structures; 2017, 24 (1), 113-128.

[23] Wijesiri Pathirana S, Uy B, Mirza O, Zhu X. Flexural behaviour of composite steel–concrete beams utilising blind bolt shear connectors. Engineering Structures; 2016, 114, p.181-194.

[24] Rehman N, Lam D, Dai X, Ashour A. Experimental study on demountable shear connectors in composite slabs with profiled decking. Journal of Constructional Steel Research; 2016, 122, p.178-189.

[25] Shim C, Lee P, Chang S. Design of shear connection in composite steel and concrete bridges with precast decks. Journal of Constructional Steel Research; 2001, 57(3), p.203-219.

[26] Shim C, Lee P, Kim D, Chung C. Effects of Group Arrangement on the Ultimate Strength of Stud Shear Connection. In: International Conference on Composite Construction in Steel and Concrete 2008. American Society of Civil Engineers; 2008, p.92-101.

[27] Smith A, Couchman G. Strength and ductility of headed stud shear connectors in profiled steel sheeting. Journal of Constructional Steel Research; 2010, 66(6), p.748-754.

[28] Nguyen H, Kim S. Finite element modeling of push-out tests for large stud shear connectors. Journal of Constructional Steel Research; 2009, 65(10-11), p.1909-1920.

[29] Anandavalli N, Rajasankar J, Prakash A, Sivaprasad B. Static Response of Steel-Concrete-Steel Sandwich Beam with Bi-Directionally Inclined Connectors. American Journal of Civil Engineering and Architecture; 2013, 1(1), p.15-20.

[30] Haghinejada A, Nematzadeh M. Three-Dimensional Finite Element Analysis of Compressive Behavior of Circular Steel Tube-Confined Concrete Stub Columns by New Confinement Relationships. Lat. Am. j. solids struct; 2016, 13(5), p.916-944.

[31] Griffin D. Design of Precast Composite Steel-Concrete Panels for Track Support: For Use on the Sydney Harbour Bridge. bachelor. University of Western Sydney; 2013.

[32] Griffin D WP, Mirza O, Kwok K, Kaewunruen S. Composites for railway construction and maintenance: A mechanistic review, The IES Journal Part A: Civil & Structural Engineering; 2014.

[33] Griffin D W P, Mirza O, Kwok K, Kaewunruen S. Finite element modelling of modular precast composites for railway track support structure – A battle to save Sydney Harbour Bridge, Australian Journal of Structural Engineering; 2015, 16(2): 150-168.

[34] Wakui H, Okuda H. A study on limit-state design for prestressed concrete sleepers.Concrete Library of JSCE; 1999, 33, p.1-25.

[35] Forni D, Chiaia B, Cadoni E. Strain rate behaviour in tension of S355 steel: Base for progressive collapse analysis. Engineering Structures; 2016, 119, p.164-173.

[36] Macri, S., Devic, A. and Asmaro, S. (2015). *Sydney Harbour Bridge: Railway Impact Loadings on Composite Steel-Concrete Transoms*. Bachelor. University of Western Sydney.

[37] Kaewunruen, S., Sussman, J.M., and Matsumoto, A., (2016). Grand Challenges in Transportation and Transit Systems. Front. Built Environ. 2:4. doi: 10.3389/fbuil.2016.00004